Advanced Fiber Materials (2020) 2:265–278
https://doi.org/10.1007/s42765-020-00046-8

RESEARCH ARTICLE

Facile and Low-Cost Fabrication of a Thread/Paper-Based Wearable System for Simultaneous Detection of Lactate and pH in Human Sweat

Gang Xiao[1] · Jing He[1] · Yan Qiao[1] · Feng Wang[2,3] · Qingyou Xia[2,3] · Xin Wang[4] · Ling Yu[1] · Zhisong Lu[1] · Chang-Ming Li[1,5]

Received: 28 February 2020 / Accepted: 3 June 2020 / Published online: 23 June 2020

Abstract

Wearable devices have received tremendous interests in human sweat analysis in the past few years. However, the widely used polymeric substrates and the layer-by-layer stacking structures greatly influence the cost-efficiency, conformability and breathability of the devices, further hindering their practical applications. Herein, we report a facile and low-cost strategy for the fabrication of a skin-friendly thread/paper-based wearable system consisting of a sweat reservoir and a multi-sensing component for simultaneous in situ analysis of sweat pH and lactate. In the system, hydrophilic silk thread serves as the micro-channel to guide the liquid flow. Filter papers were functionalized to prepare colorimetric sensors for lactate and pH. The smartphone-based quantitative analysis shows that the sensors are sensitive and reliable. Although pH may interfere the lactate detection, the pH detected simultaneously could be employed to correct the measured data for the achievement of a precise lactate level. After being integrated with a hydrophobic arm guard, the system was successfully used for the on-body measurement of pH and lactate in the sweats secreted from the volunteers. This low-cost, easy-to-fabricate, light-weight and flexible thread/paper-based microfluidic sensing device may hold great potentials as a wearable system in human sweat analysis and point-of-care diagnostics.

Keywords Wearable sensors · Thread/paper-based microfluidics · Sweat analysis · Point-of-care diagnostics · Multi-sensing system

Introduction

Skin is the soft outer covering the whole human body that protects us from pathogenic microbes and harmful elements in the ambient environment. On its surface, vital biological signals including body temperature, heart rate, blood pressure, and biopotentials could be monitored for the assessment of the overall health [1–3]. In order to grasp the health status more accurately, it is necessary to have deeper information at the molecular level. Sweat is a biofluid produced by the eccrine glands, which can be secreted to the skin surface via the dermal ducts for the regulation of body temperature. During the sweat secretion, a variety of biomarkers including ions, biometabolites, hormones and peptides are absorbed into sweat from the surrounding cells and the interstitial fluid [4]. It has been reported that sweat lactate concentration is closely correlated to the exercise intensity and tissue hypoxia degree [5, 6]. Sweat pH is also an indicator relevant to body hydration, which is critical for the fitness as well as the skin diseases [7]. Therefore, monitoring of sweat

Electronic supplementary material The online version of this article (https://doi.org/10.1007/s42765-020-00046-8) contains supplementary material, which is available to authorized users.

✉ Ling Yu
lingyu12@swu.edu.cn

✉ Zhisong Lu
zslu@swu.edu.cn

1 Institute for Clean Energy and Advanced Materials, School of Materials and Energy, Southwest University, 1 Tiansheng Road, Chongqing 400715, People's Republic of China

2 State Key Laboratory of Silkworm Genome Biology, Southwest University, 1 Tiansheng Road, Chongqing 400715, People's Republic of China

3 Chongqing Engineering and Technology Research Center for Novel Silk Materials, Southwest University, 1 Tiansheng Road, Chongqing 400715, People's Republic of China

4 College of Food Science, Southwest University, No. 2 Tiansheng Road, Beibei District, , Chongqing 400715, People's Republic of China

5 Institute of Advanced Cross-Field Science, Qingdao University, Qingdao 266071, People's Republic of China

lactate and pH should be of great importance to assess the physiological status of human body under high-temperature environment or during vigorous exercise.

Wearable sensing devices are ideal for the sweat analysis because of their flexibility and conformability with skin, allowing for the close attachment to the sweat generation sites [8, 9]. In the past few years, many wearable systems have been developed for the analysis of glucose, lactate, chloride ions, sodium ions, calcium ions, ethanol and caffeine in human sweat [10, 11]. Among them, various polymers, such as polydimethylsiloxane (PDMS) [12, 13], poly(methyl methacrylate) (PMMA) [14], silicon wafer [15] and biomedical adhesives, are usually utilized as skin-contacted substrates to fabricate patch-type wearable microfluidic sensors via sequential stacking of microchannel, active and covering layers. Generally, a complex micro-fabrication process and expensive instruments are needed to precisely control the locations and sizes of the microchannels and the holes in each layer. Special attentions should also be paid to the integration of the devices to avoid the mismatch of the holes and the channels in the neighbored layers. The layer-by-layer deposition of functional layers on the substrates may raise the thickness of the patches, further affecting the conformability to the human skin and the mechanical tolerance to repeated body motions [16, 17]. Moreover, the polymeric substrates are normally impermeable to gas and humidity, which may remarkably hinder the natural breath of human skin. Undoubtedly, the above drawbacks greatly limit the practical applications of the patch-type wearable sensing devices in sweat analysis. It is highly desirable to design a low-cost and easy-to-fabricate wearable system with excellent flexibility, great skin-conformability and superior gas-permeability for the on-body sweat analysis during vigorous exercise.

Thread, a material twisted by two or more filaments, has a long history in textile industry. Recently, it has been used as a versatile material for the fabrication of microfluidic diagnostic systems due to its low cost, good flexibility, light weight, and excellent liquid wicking ability [18, 19]. The gaps between the twisted filaments can function as capillary channels to transport liquids along the thread without external pumps [20–22]. In comparison to the conventional microfluidics, the liquid can be definitely confined in the thread region without the need to construct micro-scale channels and hydrophobic barriers [23]. Moreover, the basic microfluidic functions like mixing, separation and networking could be achieved through twisting and knotting of several threads [24–26]. Due to the great advantages, the thread-based microfluidic systems have been designed to rapidly type blood samples and detect proteins/nucleic acid [27–29]. As the building block of clothes, thread fulfils the requirements of wearable devices on flexibility and skin-affinity. It could be incorporated in the next-to-skin clothing via sewing, weaving, knotting and stitching [30]. Very hydrophilic cotton yarns have been stitched on the superhydrophobic textile substrates to produce the fluidic networks for the high-efficient sweat transport and removal from the artificial skin [31, 32].

The filter paper is composed of disorderly stacking cellulose fibers with abundant hydroxyl (–OH) active groups, which render it a very promising substrate for the immobilization of bioactive substances. Recently, filter papers have been successfully used as the substrates to adsorb enzymes and reagent molecules for the fabrication of various types of paper-based colorimetric sensors [27]. Hydrophilic thread has also been incorporated with paper-based colorimetric sensors to fabricate microfluidic platforms for quantitative detection of glucose, nitrite ions and uric acid [33–35]. Since both thread and filter paper possess excellent flexibility, air permeability, and biodegradability, the microfluidic thread/paper-based analytical device (μTPAD) could be integrated with textiles to prepare wearable systems for human sweat analysis.

Herein, a low-cost, highly conformable and skin-friendly wearable system was fabricated using very simple tools, a needle and a pair of scissors, for the in situ detection of lactate and pH in human sweat. The system contains cotton pads, hydrophilic silk threads and filter papers, which function as the sweat reservoir, liquid-transport microchannels and colorimetric sensors, respectively. To achieve the transport of sweat from the reservoir to the paper-based sensors, two hydrophilic silk threads are twisted and knotted to form a Y-shaped structure for efficient separation of the liquid sample. For easy signal readout, a homemade smartphone-based platform was established to capture images and quantitatively analyze the color change caused by the analytes. After evaluating its sensing performance with artificial sweat, the system was integrated with an arm guard to demonstrate its capability for non-invasive in situ monitoring of lactate and pH in sweat perspired from volunteers during severe exercise.

Experimental Section

Materials and Reagents

Lactic acid (85 wt% in H_2O), lactate colorimetric assay kit containing assay buffer, enzyme mix, substrate mix and lactate standard, and Whatman@ filter paper (pure cellulose paper, Grade 1) were purchased from Sigma-Aldrich (Shanghai, China). Universal pH indicator solution (in isopropanol, the pH sensing range 3.0–10.0), urea and acetic acid were bought from Adams-beta Co. Ltd (Shanghai, China). Glucose, uric acid, ascorbic acid, NaCl, NH_4Cl, and NaOH purchased from the Aladdin Chemical Reagent Co.,

Ltd. (Shanghai, China). All other reagents were of analytical grade and directly used in the present study without further purifications. Deionized water was generated by a Millipore water purification system.

The smooth surface of the Nylon fibers may lead to the yarn untwisting in the sewing and device fabrication process. Natural cotton thread needs pre-treatment to remove the wax on the surface of cellulose. In the present work, we chose super-hydrophilic silk thread provided by State Key Laboratory of Silkworm Genome Biology (Southwest University, Chongqing, China) to serve as the flow channels. The silk thread can be used directly and the hydrophilicity could be maintained for a long time. Superhydrophilic cotton pads are produced by Unicharm, Japan.

Design of μTPAD for Human Sweat Analysis

As shown in Scheme 1, the microfluidic thread/paper-based analytical device (μTPAD) contains a sweat reservoir and a microfluidic sensing component. Two cotton pads and a thread form the sweat reservoir, which can store human sweat at a volume of 31.5 ± 2.0 μL for immediate analysis. A 1.0 cm × 0.5 cm cotton pad and a 0.2 cm × 0.3 cm cotton pad are fixed on two sides of a hydrophobic fabric, respectively. The former directly contacts with skin to effectively harvest the sweat secreted from human body. The latter exposes to the outer environment for easy linking up with the microfluidic sensing component. A silk thread is sewed across the fabric with the jersey stitch method to connect the two pads, guiding the sweat from the skin side to the outer side. A double-sided adhesive is used as a substrate for the fabrication of a thread-based microfluidic sensing component. Two pieces of functionalized filter papers are attached abreast on the double-sided adhesive to serve as colorimetric sensors for lactate and pH, respectively. Two silk threads are twisted to produce a Y-shaped structure, in which the bifurcated ends are in contact with the filter papers. The rest end of the twisted threads passes through the adhesive tape, connecting with the 0.2 cm × 0.3 cm cotton pad. In practical application, the sweat reservoir and the adhesive tape-based sensing component are linked up via the connecting pads to allow the sweat flowing from the absorbent cotton pad to the filter papers. The connecting pad on the sensing component was located at the border of the lower surface of a double-side tape so that its edge could be easily seen from above. When we fix the sensing component, the upper and bottom connecting pads could be matched very well to ensure the good connection between the components.

Fabrication of Paper-Based Lactate and pH Sensors

Filter papers were cut into small round pieces with the diameter of 5 mm. To ensure the high-performance lactase sensing, a Lactase Assay Kit was employed to prepare the filter paper-based colorimetric sensor. In brief, the enzyme mix, substrate mix and assay buffer in the kit were successively dropped onto a filter paper at the volume of 3, 2.5 and 3 μL, respectively, followed by air-drying for ~ 10 min. The principle for the lactate detection is shown as below:

$$Lactate + O_2 \overset{hydrogenase}{\rightarrow} Pyruvate + H_2O_2,$$

$$H_2O_2 \rightarrow O_2 + 2H^+ + 2e^-.$$

With the assistance of lactate hydrogenase, lactate is oxidized to form hydrogen peroxide, which reacts with the substrates to generate colorimetric products. As to the pH sensor, 3 μL of Universal pH Indicator containing 100 μM NaOH was dropped onto a filter paper, drying at room temperature for ~ 10 min. The color of the Universal pH Indicator can change from red to green in the pH range of 3.0–10.0.

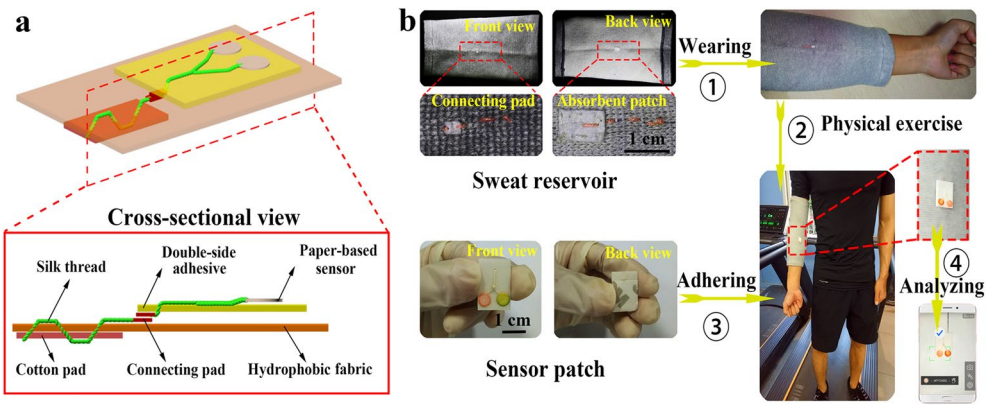

Scheme 1 Design of a thread/paper-based wearable system coupled with a smartphone for in-situ sweat analysis

The functionalized papers were stored at 4 °C and directly used in the following experiments.

Preparation of Artificial Sweat

Artificial sweat was prepared according to the standard ISO 3160-2, containing 20 g/L NaCl, 17.5 g/L NH_4OH, 5 g/L acetic acid and 15 g/L lactate [36]. The pH of the artificial sweat was adjusted to 4.0, 5.0, 6.0, 7.0, and 8.0 with 0.1 mM NaOH or 0.1 mM HCl. To obtain samples containing various concentrations of lactate, different amount of lactate powder was spiked into the artificial sweat without changing the amounts of the other reagents. During the measurements, the artificial sweat was added onto the cotton absorbent pads, followed by an incubation at room temperature for 10 min. The liquid wicks into the thread and gradually flows to the paper-based sensing components, resulting in the color changes of the filter papers. All experiments were conducted at room temperature (20–25 °C).

Signal Readout with a Smartphone-Based System

A smartphone-compatible light shielding box was manufactured with the 3D printing technique to avoid the light interference from the environment (Fig. S1 in ESI). The smartphone's build-in light source and camera were applied to collect the images of the paper-based sensors. The RGB values were obtained with a smartphone-based software (Color Grab, Loomatix Ltd.) to quantitatively evaluate the color change caused by the analytes in sweat.

On-Body Sweat Collection and Analysis

The sweat reservoir was sewed on a hydrophobic arm guard according to our design for on-site collection of human sweat. We chose an arm guard to incorporate the as-prepared wearable system because of the following two reasons: (1) the arm normally perspires faster than the rest of the body surface [37, 38]; (2) it should be much easier for the wearer to replace the sensing component located at the arm rather than back, forehead and leg. The system could also be integrated with clothing to analyze sweat secreted from other parts of human body according to the practical requirements. The adhesive tape-based sensing component was exactly adhered to ensure the liquid flow along the thread from the sweat reservoir to the sensors. The adhesive tape-based part can be replaced during the practical applications to achieve continuous monitoring of human sweat. Four healthy male volunteers were selected to wear the arm guard during exercise. Their sweats were in-situ analyzed after 10, 25 and 40 min of running to demonstrate the capability of the device for on-body measurement. After each test, the tape-based part was removed from the arm guard for smartphone-based analysis. Simultaneously, tissue papers were employed to absorb sweat from the connecting pad of the reservoir. The constant updating of fresh sweat in the device can guarantee the accuracy of the next round of test. To verify the reliability of the as-prepared system, commercially available pH meter (CLEAN LEAU pH 30) and lactate colorimetric assay kit (Sigma-Aldrich) were used to measure the pH value and lactate level, respectively, in human sweat for comparison. For the sweat pH measurement, the pH tester was directly contacted with the cotton absorbent pad on the inner side of the arm guard, which harvested the sweat sample from a volunteer. As to the lactate test, the sweat was collected from the volunteer' arms and directly measured following the kit manual.

Results and Discussion

To verify the performance of the paper-based colorimetric sensors, an absorbent pad and a paper-based sensor are connected with a hydrophilic silk thread to form a simple μTPAD with a single channel for the separate detection of lactate and pH in artificial sweat. We use a homemade smartphone-based platform to analyze the experimental results and present them in a model including R, G and B values (Fig. S1 in ESI). Firstly, the same paper-based sensor with orange color was measured independently for seven times to verify the reliability of the homemade signal readout system. The standard deviations of the R, G and B values are only 1.38, 1.83 and 0.98, respectively (Fig. S2 in ESI), showing the satisfactory consistency of the smartphone-based system. Secondly, the color analysis process was performed under various light conditions to prove the significant influence of the ambient light on the RGB values obtained with the smartphone (Fig. S3 in ESI). Hence, the shielding box in the designed signal readout system is necessary for the accurate and precise color analysis of the paper-based sensors. Thirdly, the effect of capture angle on the results was also investigated. The same paper-based sensor was inserted into the shielding box at the angle of 0°, 5°, 10°, 15°, 20° and 30°, respectively, with the smartphone fixed at the top. There is no significant difference on the RGB values at the angle ranging from 0° to 10° (Fig. S4 in ESI). In the practical application, the paper-based sensor is normally placed horizontally (less than 10°) in the light shielding box, which ensures accuracy of the measurement.

In order to further verify the reproducibility of the thread/paper-based colorimetric sensing device, five artificial sweat samples with the identical lactate concentration and pH value were measured using the as-prepared devices independently. Results show that the R/G/B values maintain at quite stable levels, respectively (Fig. S5 in ESI), indicating the excellent consistency between devices. Before the

quantitative measurements of lactate and pH in artificial sweats, the preparation of the paper-based sensors was optimized by adjusting the reaction time and reagent amount to obtain the best sensing performance (Fig. S6 and S7 in ESI).

For the lactate testing, a series of artificial sweats containing different concentrations of lactate were dropped on the absorbent pads to trigger the enzyme-catalyzed color alteration. After the reaction, a noticeable color alteration can be observed from the images (Fig. 1a). As the lactate concentration increases, the color of the sensor gradually changes from orange to brown. Interestingly, it is found that the colorful substances tend to aggregate at the edge of the filter papers, forming an orange or a brown ring. This phenomenon may be caused by the continuous flow of the liquid from the thread into the paper, which carries the pre-deposited reagents to the edge of the paper. The difference on the color intensity between the sensors treated with 0 and 25 mM lactate was compared in terms of the R, G and B values, respectively. Although statistical alterations can be observed in all groups (Fig. 1b), the B value exhibits the most significant difference. Therefore, the application of B value in quantitative measurement of lactate may possibly provide the highest sensitivity to the test. As shown in Fig. 1c, the B value is negatively correlated to the lactate concentration in the range of 0 to 25 mM ($R^2 = 0.92$), which matches well with the lactate concentration (5–20 mM) in human sweat [7, 41]. The assay possesses a limit of detection of 0.98 mM (3σ/slope of the analytical curve, where σ is the standard deviation of negative control) and the sensitivity of -3.07 mM^{-1}. The results indicate that the microfluidic thread/paper-based lactate sensor could be used as a reliable device to determine the lactate concentration in human sweat.

A universal pH indicator was immobilized on the filter papers to fabricate the sensors for the sweat pH measurement. Since the original color of the indicator is orange, the reaction cannot induce obvious color alteration on the paper due to the weak acid/neutral nature of the human sweat (three images on the left of Fig. 2a). In order to clearly monitor the infiltration of sweat into the filter paper, a trace alkaline (100 μM NaOH) was complemented into the pH indicator solution, leading to a color change from orange to light green (three images on the right of Fig. 2a). After adding samples with pH 8.0 onto the sensor, a prominent color change from green to orange could be observed. The phenomena clearly show the efficient reaction of sweat with the pH indicator molecules in the filter paper-based sensor (Fig. 2b). The smartphone-based analysis was further conducted to obtain the RGB values of the sensors. It can be seen from Fig. 2c that the most significant color difference between the samples with pH 4.0 and 8.0 can be obtained using the G value. Thus, for the analysis of sweat pH, G value was collected in the following experiments. The pH of human sweat has been reported to vary from 4.0 to 8.0. The performance of the thread/paper-based pH sensor was evaluated with artificial sweats at pH 4.0, 5.0, 6.0, 7.0 and 8.0, respectively. The inset images in Fig. 2d show the sensor colors after reactions. There is a linear correlation between the G value and the sweat pH in the range from pH 4.0 to 8.0 with R^2 of 0.99 and the sensitivity of 10.43. Because the dynamic range and the sensitivity can meet the requirements of the pH measurement in human sweat, the as-prepared pH sensing component was incorporated with the above-tested lactate sensor to prepare the multi-sensing component for human sweat analysis.

Sweat contains a wealth of chemical information that could possibly interfere with the colorimetric sensing. In

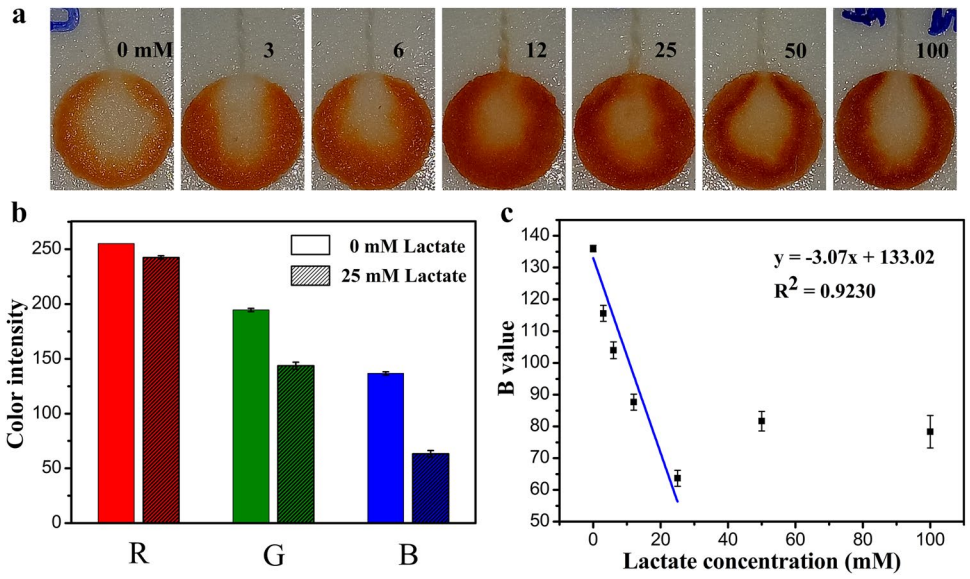

Fig. 1 **a** Thread/paper-based lactate sensors after reacting with artificial sweat samples containing 0, 3, 6, 12, 25, 50 and 100 mM lactate, respectively; **b** R, G and B values of the sensors after measuring artificial sweat samples (pH 6.0) containing 0 and 25 mM lactate, respectively; **c** Plots of B value against lactate concentration in artificial sweat. The data obtained from three independent experiments are presented as the mean ± standard deviations

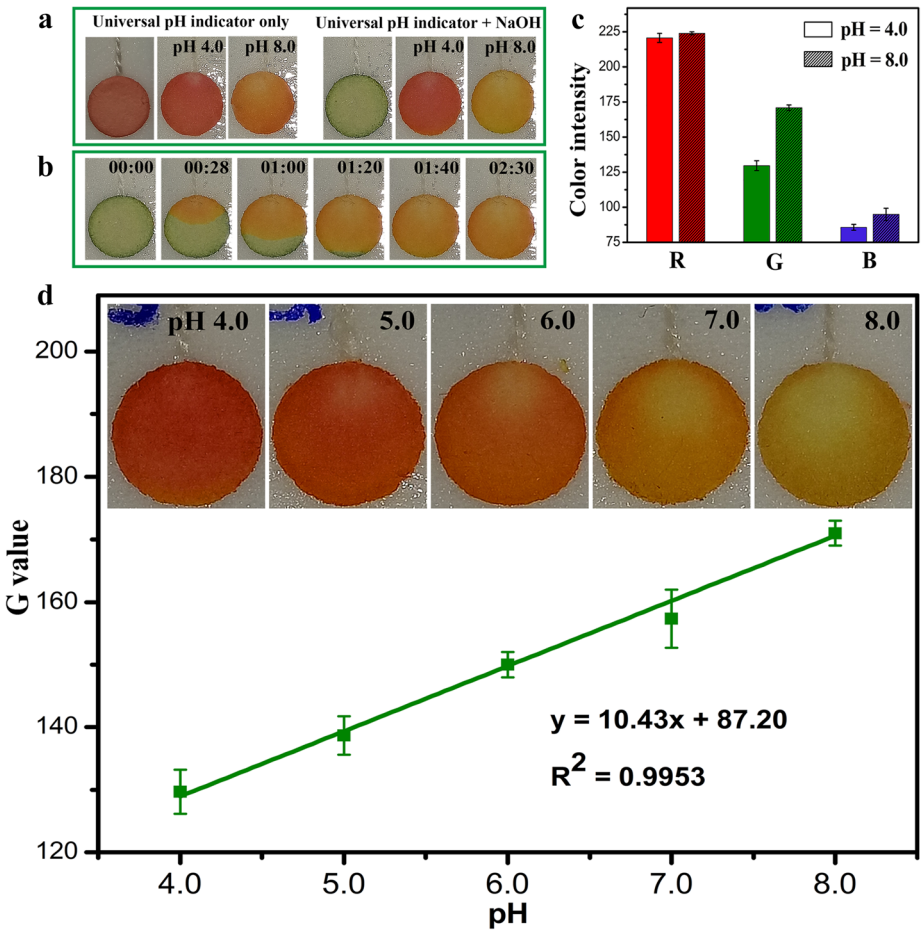

Fig. 2 **a** Thread/paper-based pH sensors before/after measuring artificial sweats at pH 4.0 and pH 8.0, respectively; Left: Sensors prepared with universal pH indicator only; Right: Sensors prepared with universal pH indicator + 100 μM NaOH; **b** The color-changing process during the measurement of an artificial sweat sample with a pH of 8.0; **c** R, G and B values of the thread/paper-based pH sensors after measuring artificial sweat samples at pH 4.0 and pH 8.0, respectively; **d** Plots of G value against pH value of the artificial sweat. Insets show the digital images of the thread/paper-based pH sensors after reacting with artificial sweats at pH values of 4.0, 5.0, 6.0, 7.0 and 8.0, respectively. The data obtained from three independent experiments are presented as the mean ± standard deviations

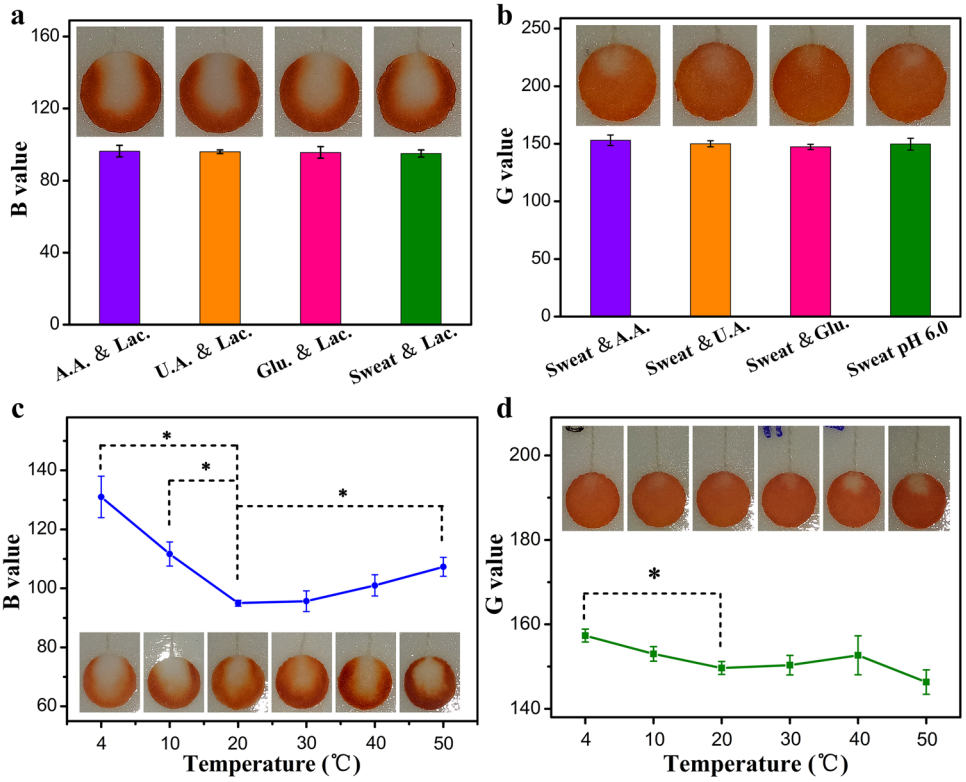

Fig. 3 Interferences of 50 μM ascorbic acid (A.A.), 50 μM uric acid (U.A.) and 200 μM Glucose (Glu.) on the colorimetric measurement of lactate (**a**) and pH (**b**) in the artificial sweat samples; Effects of ambient temperature on colorimetric measurement of lactate (**c**) and pH (**d**) in the artificial sweat samples. The data obtained from three independent experiments are presented as the mean ± standard deviations. *$p < 0.05$, two-tailed t-test, in comparison to the 20 °C group

the present study, interferences of several main components, including ascorbic acid, uric acid and glucose, on the colorimetric measurements of lactate and pH in human sweat were explored. It should be noted that all those components were spiked into the artificial sweat at the concentrations normally found in the healthy human sweat [40, 41]. As shown in Fig. 3a, b, the presence of ascorbic acid (50 μM), uric acid (50 μM), and glucose (200 mM) does not significantly affect the thread/paper device-based sensing of lactate and pH in artificial sweat, respectively. Even with the changes of other components in human sweat, the as-prepared system could still provide reliable lactate and pH data. As is well known, the rate of an enzyme-catalyzed reaction greatly relies on the temperature. The ambient temperature may possibly influence the performance of the as-prepared sweat sensors, in particular the lactate sensor. Since the dynamic curves in Figs. 1 and 2 were obtained at room temperature (20–25 °C), the 20 °C group was selected as the control to estimate effects of ambient temperature on measurements for both lactate and pH. As expected, statistical difference on B value ($p < 0.05$, in comparison to the 20 °C group) can be observed at 4, 10 and 50 °C for the lactate sensing. In the temperature range of 20–40 °C, the color intensity is maintained at a stable level (Fig. 3c). As to the pH detection, the G value keeps stable in a wide temperature range (10–50 °C) (Fig. 3d). The experimental data strongly suggest that the as-prepared lactate and pH sensing system could be practically used for human sweat analysis under normal circumstances.

Since the orientation of a clothing-attached device may change greatly in the process of wearer's movements, effects of the orientation on the sweat flow in the thread channels should be investigated before the practical use. A cotton reservoir, a connecting pad and the thread were woven into a hydrophobic fabric according to the design in Scheme 1. To avoid the liquid filtration into the fabric during the transfer process, the wearable system should be prepared with hydrophilic threads and a hydrophobic fabric. The contact angles of the silk thread and the fabric are $45.6° \pm 6.5°$ and $132.7° \pm 1.5°$, respectively (Fig. 4a), showing their distinct wettability. A double-sided adhesive is used as a substrate for the fabrication of the removable sensing patch. A connecting pad and two sensing components were adhered on each side of the substrate. Two threads were twisted and knotted to form a Y-shape channel for the connecting of the connecting pad and the two paper-based sensing components. The lengths of the thread from the cotton reservoir to the connecting pad, from the connecting pad to the knot, and from the knot to the filter paper are 1.0, 0.8 and 0.5 cm, respectively (Fig. 4c). Additionally, the cost of the skin patch is quite low (about US $ 0.37) because it is made of inexpensive materials like papers and adhesive tapes. The time for the dye moving from the reservoir to the paper was recorded to represent the flowing capability of liquids in the thread-based channels woven in the fabric (Fig. 4c–f). The devices placed vertically with the sensors up and down have the flowing time of 211.0 ± 43.7 and 183.3 ± 31.8 s, respectively. For the devices placed horizontally with the sensors toward left and right, the flowing durations are 193.3 ± 27.5 and 190 ± 17.6 s, respectively (Fig. 4h). Statistical analysis indicates that the change of the device orientations does not

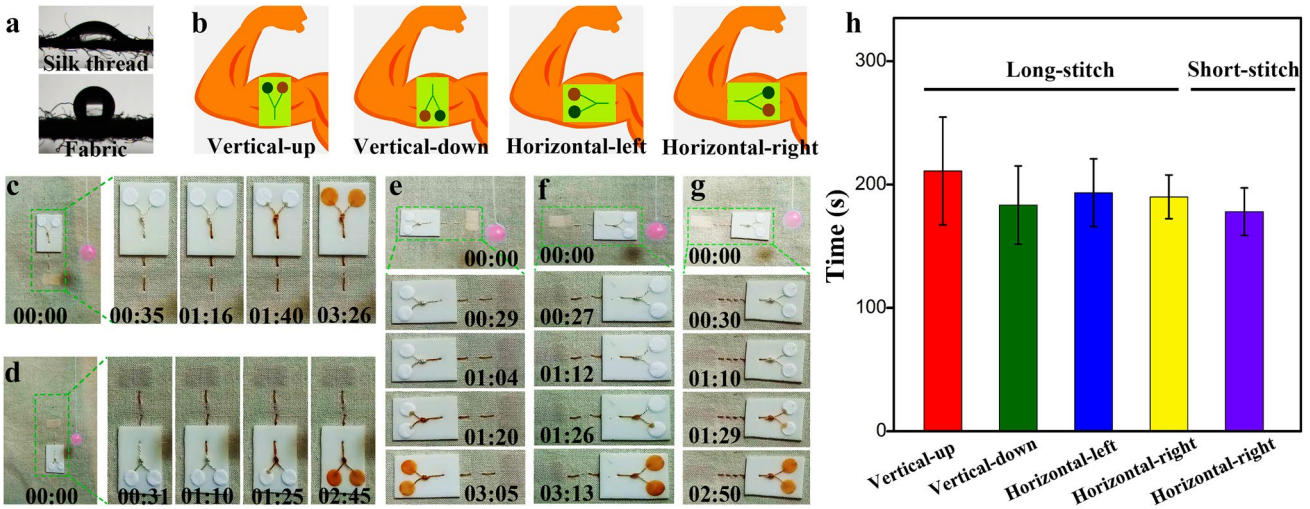

Fig. 4 **a** Contact angle images corresponding to the hydrophilic silk threads and the hydrophobic fabric. **b** Illustration of the different orientations of the microfluidic thread/paper-based devices; **c**–**g** A series of images extracted from a video illustrating transport of brown dye from the reservoir pad to the paper sensing components (The pink pendant was utilized as a reference object in the images); From **c** to **f**: Vertical-up, vertical-down, horizontal-left and horizontal-right placement, respectively; **g** Horizontal-right placement of a device sewed with a short-stitch method; **h** Duration for the transport of the dye from the reservoir pad to the paper sensing component. The data obtained from three independent experiments are presented as the mean ± standard deviations

cause significant alteration on the liquid flowing capability. Meanwhile, the connecting pads located on the sweat reservoir and the sensing component could tightly link up to efficiently transfer the liquid (Fig. 4c–g and Fig. S8 in ESI). We also considered the effect of the stitch method on the liquid transport rate. As shown in Fig. 4f, g, the thread sewed in the fabric with the short-stitch manner also does not obviously change the liquid flowing time in comparison to the one prepared with long-stitch approach. It has been reported that the liquid flow is tightly associated with the orientation and shape of the thread due to the existence of gravity and the channel size among the fibers [42, 43]. Although the vertical-up and vertical down groups show the slowest and fastest average flow velocity, respectively, there is no statistically significant difference among all groups. This phenomenon may be due to the relatively short length (2.3 cm) of the thread-based channel and variation of each thread. On the basis of the findings, it can be concluded that the flowing capability of the thread is not affected by the orientation and the stitch method in our system. The response time of the as-prepared system contains the sweat transport time and the color development time, which are measured to be ~ 3.2 min and 10.0 min, respectively (Fig. S9 in ESI). Therefore, the total response time of the system should be about 13.2 min.

The liquid storage capacity of the sweat reservoir, the dead volume of the Y-shaped microfluidic thread and the volume required for the tape-based sensing component were measured as 31.5 ± 2.0, 5.8 ± 0.4 and 13.5 ± 0.9 μL, respectively, by weighing the mass enhancement of the devices after saturation with pure water (Fig. S10 in ESI). The sweat stored in the reservoir is more than 2.3 times of the volume required for the pH and lactate sensing. Various factors should be taken into account in the dimension design of each component in the system. For the sensing paper, its shape and size should match analyzing zone of the smartphone-based software. The liquid storage capability and the time needed for the color development should also be involved in the design of the sensing component. As to the reservoir, the human perspiration rate, liquid storage capability of the cotton pad, the sweat volume needed for the sensing component, and the skin contact location should be considered. The selection of thread is also very critical for the μTPAD. The ideal thread should have excellent wicking capability, minimal liquid residual, and great compatibility with conventional woven techniques. From dozens of threads we selected the silk thread provided by State Key Laboratory of Silkworm Genome Biology (Southwest University, China), since it has better liquid wicking property over a lot of cotton threads. Since the thread/paper-based microfluidic system was directly exposed to the ambient atmosphere, the water evaporation during the sensing process should not be neglected. The weight loss of a water-saturated reservoir coupled with a tape-based sensing component was real-time monitored at 20 and 30 °C for the estimation of water evaporated. The volume of water in the system reduces very rapidly for both 20 and 30 °C group. After 50 min, the water stored in the reservoir is depleted. In our experiments, the simultaneous measurements of pH and lactate in both artificial sweat and real human sweat were completed at 20–25 °C in 10 min, during which the loss of sweat should be identical (Fig. S11 in ESI). Thus, the pH value and lactate concentration obtained with the as-prepared system should still be accurate. However, it has to be noted that the detection time and the ambient temperature should be strictly controlled during the measurement to ensure the collection of accurate data.

In our design, the lactate and pH need to be measured simultaneously with a single device. The chemical crosstalk during the detection of multiple analytes must be identified. Firstly, a series of samples containing 0, 3, 6, 12 and 25 mM lactate at a constant pH of 6.0 were prepared to study the inference of lactate levels on the pH detection. It can be found in Fig. 5a that the measured pH values are

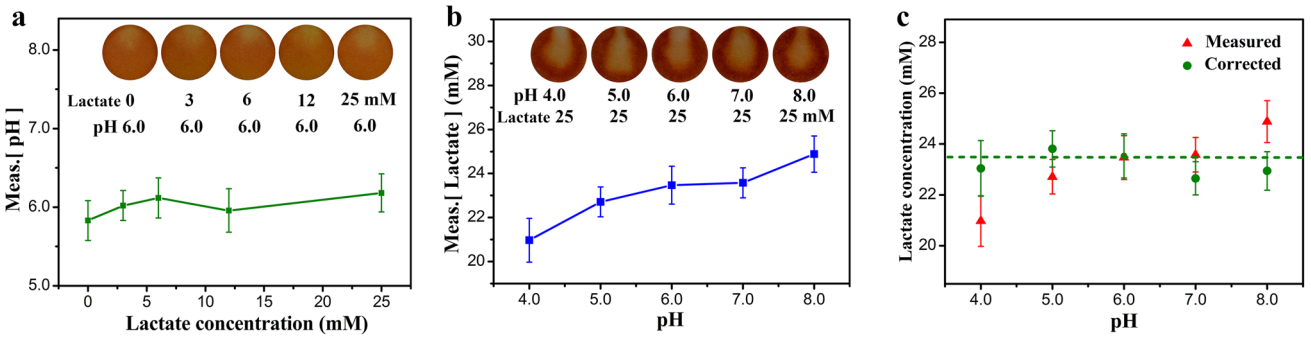

Fig. 5 **a** Effect of lactate concentration on the detection of pH value in the artificial sweat; **b** effect of pH on the detection of lactate in the artificial sweat; **c** comparison of the measured (red triangle) and corrected (green dot) lactate concentrations at different pH values. The data obtained from three independent experiments are presented as the mean ± standard deviations

quite stable without obvious deviations. The change of the lactate level does not affect the pH assay in artificial sweat. Then, a series of artificial sweats containing 25 mM lactate with the pH ranging from 4.0 to 8.0 were tested using the as-prepared microfluidic thread/paper-based multi-sensing systems, respectively. After analyzing with the smartphone and calculating based on the calibration curve, the measured lactate concentrations were plotted against pH values in Fig. 5b. The rise in the pH leads to a gradual enhancement on the measured concentration of lactate, indicating the strong interference of pH on the detection of lactate. The paper-based lactate assay is an enzyme-catalyzed reaction system, in which the enzyme activity is greatly dependent on the environment pH. The interference due to the pH change seems to be unavoidable. Actually, at different pH, the calibration curve used to calculate the lactate concentration should be distinct because of the alteration of the enzyme activity. Fortunately, there is a linear relationship between the sensitivity of the calibration curve and the sample pH value (Fig. S12). Therefore, the corrected calibration equation of lactate concentration can be calculated with the pH measured from the samples. As shown in Fig. 5c, the corrected data are much more precise than the measured ones. In order to eliminate the pH interference on the lactate sensing, the measured pH value should be employed to correct the data for the achievement of precise results in the following on-body tests. The approach was reported by Lee et al. to correct the sweat sensing results obtained with an electrochemical device [39].

To validate the reliability and accuracy of the thread/paper-based sweat analysis system, commercially available pH meter and lactate colorimetric assay kit were utilized to measure the sweat sample from the same volunteer after exercise for 10, 25 and 40 min for comparison. As shown in Table 1, comparable data could be obtained with both commercially available methods and μTPAD. The results strongly prove that the as-prepared μTPAD could be used as a reliable system for the pH and lactate analysis in human sweat. The μTPAD was fixed on a hydrophobic arm guard to further demonstrate the feasibility of the devices for in situ multicomponent analysis in human sweat. The functionalized arm guards were worn on the volunteers' left arms to perform the in situ detections. After each test, the tape-based sensing component was removed from the fabric and analyzed with the smartphone-based system immediately.

Table 1 Comparison of the sweat pH/lactate concentrations measured using commercially available approaches and the as-prepared μTPAD

Exercise time (min)	Commercially available methods	μTPAD
pH		
10	4.7	4.9
25	6.5	6.1
40	7.4	6.9
Lactate		
10	14.7 mM	16.5 mM
25	11.7 mM	12.7 mM
40	10.3 mM	8.3 mM

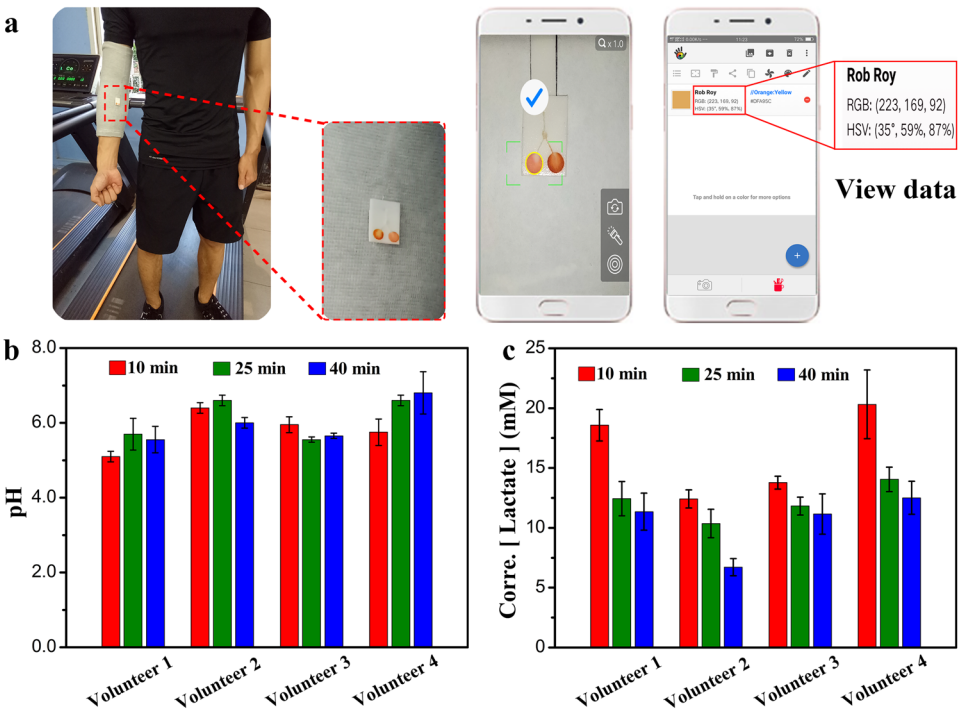

Fig. 6 **a** An arm guard-integrated device after the on-body measurement; **b** the corresponding image and data obtained with a smartphone; **c** pH values and **d** lactate concentrations for four healthy male volunteers tested after 10, 25 and 40 min of running. The data obtained from three independent experiments are presented as the mean ± standard deviations

Table 2 Wearable microfluidic sensors for colorimetric analysis of lactate and pH in human sweat

	Skin-contacted substrate	Materials for microfluidic channel fabrication	Air/humidity-permeability	Instruments for manufacturing	Data collection	Bio-degradable	Dynamic range	Limit of detection	References
Lactate	Acrylate adhesive	Silicon wafer/PMMA/PDMS	Low	Patterned mould/deep reactive ion etching/rotary coating machine/ electric drying oven	Smartphone camera/Color Reference Marker	No	5–20 mM	2 mM	[9]
	Adhesive layer	PDMS	Low	Negative photoresist SPR/reactive-ion etching/mechanical punches/Harrick plasma cleaner	Smartphone/NFC electronics	No	1.5–100 mM	0.3 mM	[12]
	Cotton fabrics	Cotton fabrics	High	Screen-printed/electrothermostatic blast oven	Camera/portable spectrophotometer	Yes	0–25 mM	–	[48]
	Cotton-silk thread	Silk thread	High	Universal pH indicator solution	Smartphone App (Color Grab)	Yes	1.0–25 mM	1.0 mM	This work
pH	Acrylate adhesive	Silicon wafer/PMMA/PDMS	Low	Patterned mould/deep reactive ion etching/rotary coating machine/electric drying oven	Smartphone camera/Color Reference Marker	No	4.5–6.5	0.1	[9]
	Adhesive	PDMS-white silicone	Low	Spin coating/baking/laser printer/CO_2 laser/plasma treating	Smartphone/NFC electronics	No	–	–	[11]
	Adhesive layer	PDMS	Low	Negative photoresist SPR/reactive-ion etching/mechanical punches/Harrick plasma cleaner	Smartphone/NFC electronics	No	5.5–8.5	–	[12]
	Adhesive	PMMA/silicon wafer	Low	Deep reactive ion etching/spin coating/corona treatment	Camera/photoshop	No	5.0–7.0	–	[14]
	PMMA	PMMA/cotton thread	Low	Laser ablation system/thermal roller laminator/arduino microcontrollers/ProEngineer package	Light photo sensor modules	No	5.0–7.0	–	[32]
	PMMA	PMMA	Low	Laser micro-machining light deck/cutting machine/thermal roller laminator	Camera	No	4.5–8.0	0.5	[36]

Table 2 (continued)

Skin-contacted substrate	Materials for microfluidic channel fabrication	Air/humidity-permeability	Instruments for manufacturing	Data collection	Bio-degradable	Dynamic range	Limit of detection	References
Adhesive tape	Adhesive tape/anion exchange/paper	Medium	–	Smartphone or camera/Image J	Yes	1.0–14.0	–	[44]
Cotton fabrics	Cotton fabrics	High	Electronics (embedded processing devices and a bluetooth radio)	Color/light sensors	Yes	4.0–10.0	0.2	[45]
Adhesive-PET	Silica microarrays	Low	Oxygen plasma	Smartphone App (Color Picker)	No	4.5–7.0	0.5	[46]
Adhesive	PDMS	Low	Spin coating/baking/laser printer/CO_2 laser/plasma treating	Smartphone camera/NFC-based electronics/color reference markers	No	4.0–7.0	–	[47]
Cotton fabrics	Cotton fabrics	High	Screen-printed/ELECTRO-thermostatic blast oven	Camera/portable spectrophotometer	Yes	1.0–14.0	–	[48]
Cotton-silk thread	Silk thread	High	–	Smartphone App (Color Grab)	Yes	4.0–8.0	–	This work

The R, G and B values are obtained to calculate the lactate concentration and pH value (Fig. 6a). During the on-body assay, the sweats secreted from the volunteers after 10, 25 and 40 min of running were analyzed by simply replacing the adhesive tape-based sensing component. To ensure the accuracy of each round of test, tissue papers were attached on the connecting pad of the reservoir for constant updating of fresh sweat during the intervals of the tests. During the exercise process, the sweat pH of four healthy subjects varies in the range from 5.1 to 6.8, which is exactly the sweat pH range of a health human (Fig. 6b). The deviation of the pH value may be attributed to the change of the perspiration rate. Simultaneously, the lactate concentrations were monitored with the same systems and the final data were corrected using the measured pH values. The lowest and the highest lactate concentrations are 6.7 ± 0.7 and 20.3 ± 2.9 mM, respectively. Both of them fall in the healthy range of sweat lactate levels (5–20 mM). Interestingly, with the proceeding of the running, a reduction trend on the lactate concentration can be observed for all volunteers (Fig. 6c). This phenomenon has also been found in a previous works and the continuous perspiration-induced dilution of lactate has been used to explain the decreasing trend [5, 7]. The as-prepared wearable sweat analysis system contains two components: the sweat reservoir and the sensing component. The former is a reusable part and the latter is a disposable component. The sweat reservoir fabricated on the arm guard can be washed and reused (Fig S13 in ESI).

Conclusions

In summary, we develop a low-cost, light-weight and skin-conformable microfluidic thread/paper-based multi-sensing system using a needle and a pair of scissors for rapid and accurate in situ monitoring of human sweat pH and lactate. The system consists of a liquid reservoir for sweat collection and storage as well as a colorimetric multi-sensing component for the sensitive detection. Two threads were twisted and knotted to form a Y-shaped structure for the transfer and separation of sweat samples from the reservoir to the paper-based pH and lactate sensors. During the liquid transfer process, the flowing capability in the thread is not affected by the orientation and channel shape. The pH sensor shows a linear detection range from pH 4.0 to 8.0 with the sensitivity of 10.43. The lactate sensor possesses a dynamic range from 0 to 25 mM and the sensitivity of -3.07 mM^{-1}. Both of them can be used as reliable devices for the sweat analysis. Although the detection of lactate can be influenced by the sweat pH alteration, the pH detected simultaneously could be employed to correct the measured data for the achievement of the precise lactate concentration. Finally, the great feasibility of the system for the on-body analysis

was demonstrated by in-situ measuring pH and lactate concentrations in the sweats secreted from the volunteers after 10, 25 and 40 min of running. In comparison to the existing colorimetric wearable devices for sweat analysis, the as-prepared thread/paper-based microfluidic system is much easier to be fabricated and demonstrates better conformability, air/humidity permeability, and biodegradability (Table 2). This work not only extends the applications of the thread-based microfluidic device to human sweat analysis, but also provides a very promising approach to fabricate thread-based wearable systems for point-of-care diagnostics.

Acknowledgements This work was financially supported by Chongqing Natural Science Foundation (cstc2019jcyj-msxmX0314), Fundamental Research Funds for the Central Universities (XDJK2019B002) and Chongqing Engineering Research Center for Micro-Nano Biomedical Materials and Devices.

Compliance with Ethical Standards

Conflict of interest The authors declare that there is no conflict of interests regarding the publication of this paper.

References

1. Liu Y, Pharr M, Salvatore GA. Lab-on-skin: a review of flexible and stretchable electronics for wearable health monitoring. *ACS Nano*. **2017**;*11*:9614.
2. Mao C, Zhang H, Lu Z. Flexible and wearable electronic silk fabrics for human physiological monitoring. *Smart Mater Struct*. **2017**;*26*:095033.
3. Li B, Xiao G, Liu F, Qiao Y, Li CM, Lu Z. A flexible humidity sensor based on silk fabrics for human respiration monitoring. *J Mater Chem C*. **2018**;*6*:4549.
4. Yang Y, Gao W. Wearable and flexible electronics for continuous molecular monitoring. *Chem Soc Rev*. **2019**;*48*:1465.
5. Derbyshire PJ, Barr H, Davis F, Higson SP. Lactate in human sweat: a critical review of research to the present day. *J Physiol Sci*. **2012**;*62*:429.
6. Alam F, RoyChoudhury S, Jalal AH, Umasankar Y, Forouzanfar S, Akter N, Bhansali S, Pala N. Lactate biosensing: the emerging point-of-care and personal health monitoring. *Biosens Bioelectron*. **2018**;*117*:818.
7. Anastasova S, Crewther B, Bembnowicz P, Curto V, Ip HM, Rosa B, Yang GZ. A wearable multisensing patch for continuous sweat monitoring. *Biosens Bioelectron*. **2017**;*93*:139.
8. Lee HB, Meeseepong M, Trung T, Kim BY, Lee NE. A wearable lab-on-a-patch platform with stretchable nanostructured biosensor for non-invasive immunodetection of biomarker in sweat. *Biosens Bioelectron*. **2020**;*156*:112133.
9. Choi J, Bandodkar AJ, Reeder JT, Ray TR, Turnquist A, Kim SB, Nyberg N, Hourlier-Fargette A, Model JB, Aranyosi AJ, Xu S, Ghaffari R, Rogers JA. Soft, skin-integrated multifunctional microfluidic systems for accurate colorimetric analysis of sweat biomarkers and temperature. *ACS Sens*. **2019**;*4*:379.
10. Gao W, Emaminejad S, Nyein HYY, Challa S, Chen K, Peck A, Fahad HM, Ota H, Shiraki H, Kiriya D, Lien D-H, Brooks GA, Davis RW, Javey A. Fully integrated wearable sensor arrays for multiplexed in situ perspiration analysis. *Nature*. **2016**;*529*:509.
11. Tai L-C, Gao W, Chao M, Bariya M, Ngo QP, Shahpar Z, Nyein HYY, Park H, Sun J, Jung Y, Wu E, Fahad HM, Lien D-H, Ota H, Cho G, Javey A. Methylxanthine drug monitoring with wearable sweat sensors. *Adv Mater*. **2018**;*30*:1707442.
12. Koh A, Kang D, Xue Y, Lee S, Pielak RM, Kim J, Hwang T, Min S, Banks A, Bastien P, Manco MC, Wang L, Ammann KR, Jang K-I, Won P, Han S, Ghaffari R, Paik U, Slepian MJ, Balooch G, Huang Y, Rogers JA. A soft, wearable microfluidic device for the capture, storage, and colorimetric sensing of sweat. *Sci Transl Med*. **2016**;*8*:366ra165.
13. Xiao J, Liu Y, Su L, Zhao D, Zhao L, Zhang X. Microfluidic chip-based wearable colorimetric sensor for simple and facile detection of sweat glucose. *Anal Chem*. **2019**;*91*:14803.
14. Zhang Y, Guo H, Kim SB, Wu Y, Ostojich D, Park SH, Wang X, Weng Z, Li R, Bandodkar AJ, Sekine Y, Choi J, Xu S, Quaggin S, Ghaffari R, Rogers JA. Passive sweat collection and colorimetric analysis of biomarkers relevant to kidney disorders using a soft microfluidic system. *Lab Chip*. **2019**;*19*:1545.
15. Sekine Y, Kim SB, Zhang Y, Bandodkar AJ, Xu S, Choi J, Irie M, Ray TR, Kohli P, Kozai N, Sugita T, Wu Y, Lee K, Lee K-T, Ghaffari R, Rogers JA. A fluorometric skin-interfaced microfluidic device and smartphone imaging module for in situ quantitative analysis of sweat chemistry. *Lab Chip*. **2018**;*18*:2178.
16. Martín A, Kim J, Kurniawan JF, Sempionatto JR, Moreto JR, Tang G, Campbell AS, Shin A, Lee MY, Liu X, Wang J. Epidermal microfluidic electrochemical detection system: enhanced sweat sampling and metabolite detection. *ACS Sens*. **2017**;*2*:1860.
17. Lin H, Zhao Y, Lin S, Wang B, Yeung C, Cheng X, Wang Z, Cai T, Yu W, King K, Tan J, Salahi K, Hojaiji H, Emaminejad S. A rapid and low-cost fabrication and integration scheme to render 3D microfluidic architectures for wearable biofluid sampling, manipulation, and sensing. *Lab Chip*. **2019**;*19*:2844.
18. Weng X, Kang Y, Guo Q, Peng B, Jiang H. Recent advances in thread-based microfluidics for diagnostic applications. *Biosens Bioelectron*. **2019**;*132*:171.
19. Tian T, Li J, Song Y, Zhou L, Zhu Z, Yang CJ. Distance-based microfluidic quantitative detection methods for point-of-care testing. *Lab Chip*. **2016**;*16*:1139.
20. Cabot JM, Breadmore MC, Paull B. Thread based electrofluidic platform for direct metabolite analysis in complex samples. *Anal Chim Acta*. **2018**;*1000*:283.
21. Mousavi MPS, Ainla A, Tan EKW, Abd El-Rahman M, Yoshida Y, Yuan L, Sigurslid HH, Arkan N, Yip MC, Abrahamsson CK, Homer-Vanniasinkam S, Whitesides GM. Ion sensing with thread-based potentiometric electrodes. *Lab Chip*. **2018**;*18*:2279.
22. Agustini D, Bergamini MF, Marcolino-Junior LH. Tear glucose detection combining microfluidic thread based device, amperometric biosensor and microflow injection analysis. *Biosens Bioelectron*. **2017**;*98*:161.
23. Reches M, Mirica KA, Dasgupta R, Dickey MD, Butte MJ, Whitesides GM. Thread as a matrix for biomedical assays. *ACS Appl Mater Inter*. **2010**;*2*:1722.
24. Ulum MF, Maylina L, Noviana D, Wicaksono DHB. EDTA-treated cotton-thread microfluidic device used for one-step whole blood plasma separation and assay. *Lab Chip*. **2016**;*16*:1492.
25. Ramesan S, Rezk AR, Cheng KW, Chan PPY, Yeo LY. Acoustically-driven thread-based tuneable gradient generators. *Lab Chip*. **2016**;*16*:2820.
26. Safavieh R, Zhou GZ, Juncker D. Microfluidics made of yarns and knots: from fundamental properties to simple networks and operations. *Lab Chip*. **2011**;*11*:2618.
27. Erenas MM, Carrillo-Aguilera B, Cantrell K, Gonzalez-Chocano S, Perez de Vargas-Sansalvador IM, de Orbe-Payá I, Capitan-Vallvey LF. Real time monitoring of glucose in whole blood by smartphone. **Biosens Bioelectron**. **2019**;*136*:47.

28. Mao X, Du T-E, Wang Y, Meng L. Disposable dry-reagent cotton thread-based point-of-care diagnosis devices for protein and nucleic acid test. *Biosens Bioelectron*. **2015**;*65*:390.
29. Wu T, Xu T, Xu L-P, Huang Y, Shi W, Wen Y, Zhang X. Superhydrophilic cotton thread with temperature-dependent pattern for sensitive nucleic acid detection. *Biosens Bioelectron*. **2016**;*86*:951.
30. Mostafalu P, Akbari M, Alberti KA, Xu Q, Khademhosseini A, Sonkusale SR. A toolkit of thread-based microfluidics, sensors, and electronics for 3D tissue embedding for medical diagnostics. *Microsyst Nanoeng*. **2016**;*2*:16039.
31. Xing S, Jiang J, Pan T. Interfacial microfluidic transport on micropatterned superhydrophobic textile. *Lab Chip*. **2013**;*13*:1937.
32. Curto VF, Coyle S, Byrne R, Angelov N, Diamond D, Benito-Lopez F. Concept and development of an autonomous wearable micro-fluidic platform for real time pH sweat analysis. *Sens Actuators B Chem*. **2012**;*175*:263.
33. Gonzalez A, Estala L, Gaines M, Gomez FA. Mixed thread/paper-based microfluidic chips as a platform for glucose assays. *Electroanalysis*. **2016**;*37*:1685.
34. Li X, Tian J, Shen W. Thread as a versatile material for low-cost microfluidic diagnostics. *ACS Appl Mater Inter*. **2010**;*2*:1.
35. Xiao G, He J, Chen X, Qiao Y, Wang F, Xia Q, Yu L, Lu Z. A wearable, cotton thread/paper-based microfluidic device coupled with smartphone for sweat glucose sensing. *Cellulose*. **2019**;*26*:4553.
36. Curto VF, Fay C, Coyle S, Byrne R, O'Toole C, Barry C, Hughes S, Moyna N, Diamond D, Benito-Lopez F. Real-time sweat pH monitoring based on a wearable chemical barcode micro-fluidic platform incorporating ionic liquids. *Sens Actuators B Chem*. **2012**;*171–172*:1327.
37. Heyningen R, Weiner JS. A comparison of arm-bag sweat and body sweat. *J Physiol*. **1952**;*116*:395.
38. Matzeu G, Fay C, Vaillant A, Coyle S, Diamond D. A wearable device for monitoring sweat rates via image analysis. *IEEE Trans Biomed Eng*. **2016**;*63*:1672.
39. Lee H, Song C, Hong YS, Kim MS, Cho HR, Kang T, Shin K, Choi SH, Hyeon T, Kim D-H. Wearable/disposable sweat-based glucose monitoring device with multistage transdermal drug delivery module. *Sci Adv*. **2017**;*3*:e1601314.
40. RoyChoudhury S, Umasankar Y, Hutcheson JD, Lev-Tov HA, Kirsner RS, Bhansali S. Uricase based enzymatic biosensor for non-invasive detection of uric acid by entrapment in PVA-SbQ polymer matrix. *Electroanalysis*. **2018**;*30*:2374.
41. Bariya M, Nyein HYY, Javey A. Wearable sweat sensors. *Nat Electron*. **2018**;*1*:160.
42. Ballerini DR, Li X, Shen W. Flow control concepts for thread-based microfluidic devices. *Biomicrofluidics*. **2011**;*5*:14105.
43. Almoughni H, Gong H. Capillary flow of liquid water through yarns: a theoretical model. *Text Res J*. **2015**;*85*:722.
44. Mu X, Xin X, Fan C, Li X, Tian X, Xu KF, Zheng Z. A paper-based skin patch for the diagnostic screening of cystic fibrosis. *Chem Commun*. **2015**;*51*:6365.
45. Caldara M, Colleoni C, Guido E, Re V, Rosace G. Optical monitoring of sweat pH by a textile fabric wearable sensor based on covalently bonded litmus-3-glycidoxypropyltrimethoxysilane coating. *Sens Actuators B Chem*. **2016**;*222*:213.
46. He X, Xu T, Gu Z, Gao W, Xu L-P, Pan T, Zhang X. Flexible and superwettable bands as a platform toward sweat sampling and sensing. *Anal Chem*. **2019**;*91*:4296.
47. Bandodkar AJ, Gutruf P, Choi J, Lee KH, Sekine YJ, Reeder T, Jeang WJ, Aranyosi AJ, Lee SP, Model JB, Ghaffari R, Su CJ, Leshock JP, Ray T, Verrillo A, Thomas K, Krishnamurthi V, Han S, Kim J, Krishnan S, Hang T, Rogers JA. Battery-free, skin-interfaced microfluidic/electronic systems for simultaneous electrochemical, colorimetric, and volumetric analysis of sweat. *Sci Adv*. **2019**;*5*:eaav3294.
48. Promphet N, Rattanawaleedirojn P, Siralertmukul K, Soatthiyanon N, Potiyaraj P, Thanawattano C, Hinestroza JP, Rodthongkum N. Non-invasive textile based colorimetric sensor for the simultaneous detection of sweat pH and lactate. *Talanta*. **2019**;*192*:424.

Gang Xiao is currently studying for his PhD degree in Institute for Clean Energy & Advanced Materials, School of Materials & Energy, Southwest University, Chongqing, P. R. China. His research focuses on wetting phenomenon of biological materials and flexible wearable biosensors.

Jing He obtained her master degree at Institute for Clean Energy & Advanced Materials, School of Materials & Energy, Southwest University, Chongqing, P. R. China in 2019. Her research focuses on textile-based sweat analysis system.

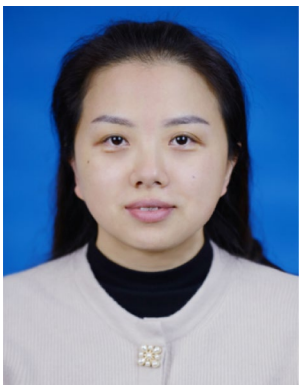

Yan Qiao is currently associate professor of the Institute for Clean Energy and Advanced Materials, School of Materials & Energy, Southwest University, Chongqing, P. R. China. She obtained her PhD degree in Bioengineering from Nanyang Technological University, Singapore in 2010. Her research focuses on bioelectrochemistry and microbial fuel cells.

Feng Wang is currently associate professor of College of Biotechnology in Southwest University, Chongqing, P. R. China. He obtained his PhD degree from Southwest University, Chongqing, P. R. China in 2014. His research interests are silk materials-based biomedical devices.

Qingyou Xia is currently professor of College of Biotechnology in Southwest University, Chongqing, P. R. China. He obtained his PhD degree from Southwest Agricultural University, Chongqing, P. R. China in 1996. He conducted 3 years post-doctoral research at KYUSHU University, Japan. His main research interests are genomics and functional genomics of silkworm, silk fibers and silk-based materials.

Xin Wang is studying for his master degree in College of Food Science, Southwest University, Chongqing, P. R. China. His research focuses on nanomaterials-based biosensors.

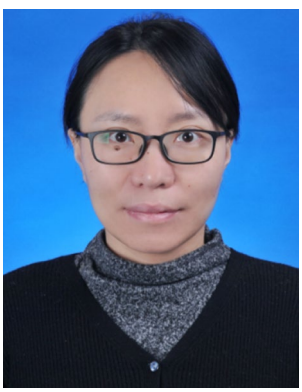

Ling Yu is currently professor of the Institute for Clean Energy and Advanced Materials, School of Materials & Energy, Southwest University, Chongqing, P. R. China. She obtained her PhD degree in Bioengineering from Nanyang Technological University, Singapore in 2009. She conducted 3 years post-doctoral research at University of Pittsburgh Medical Center, USA. Her research aims at exploring the advanced nanotechnologies and lab-on-a-chip systems for biomedical applications.

Zhisong Lu received his PhD degree in school of chemical & biomedical engineering from Nanyang Technological University, Singapore in 2011, and is currently a professor in School of Materials & Energy, Southwest University, Chongqing, P. R. China. Prof. Lu's research expertise is in smart fibers and biosensors. With an h-index of 33 and total citation of 3400, he has co-authored more than 130 papers in refereed journals and has filed 11 patents.

Chang-Ming Li is Professor and Dean of the Institute for Clean Energy and Advanced Materials in Southwest University, Chongqing, P. R. China. He worked with Motorola USA (1993–2003) as a distinguished technical member, Science Advisory Board Associate and senior manager. He was Professor, Head of Bioengineering Division and Director of Centre for Advanced Bionanosystems in Nanyang Technological University, Singapore (2003–2012). His main research interests are nanomaterials, green energies and biosensors/lab-on-a-chip systems.